

## NUMERICAL SIMULATION OF THE TRANSMISSION OF SOUND WAVES ON HOLLOW CONCRETE BLOCKS AND THEIR BEHAVIOR AS ACOUSTIC INHIBITOR.

Fabián Bastidas-Alarcón 1, Lidia Castro-Cepeda 2\* Eder Cruz-Sigüenza 3, Eugenia Naranjo-Vargas 4, Edwin Pozo-Safla 5, Luis Choto-Chariguaman 6.

- <sup>1</sup> Escuela Superior Politécnica de Chimborazo, Facultad de Mecánica, Investigation Group GISAI; [fabian.bastidas@esPOCH.edu.ec](mailto:fabian.bastidas@esPOCH.edu.ec). ORCID: 0000-0003-3238-4072
- <sup>2</sup> Escuela Superior Politécnica de Chimborazo, Facultad de Mecánica, Investigation Group GIDETER; [lidia.castro@esPOCH.edu.ec](mailto:lidia.castro@esPOCH.edu.ec) ORCID: 0000-0002-0471-2879
- <sup>3</sup> Escuela Superior Politécnica de Chimborazo, Sede Morona Santiago, Minas, Macas, Ecuador, [eder.cruz@esPOCH.edu.ec](mailto:eder.cruz@esPOCH.edu.ec) ORCID: 0000-0003-4982-9947
- <sup>4</sup> Escuela Superior Politécnica de Chimborazo, Facultad de Mecánica, Investigation Group GIDENM; [eugenia.naranjo@esPOCH.edu.ec](mailto:eugenia.naranjo@esPOCH.edu.ec) ORCID: 0000-0002-9658-6311
- <sup>5</sup> Escuela Superior Politécnica de Chimborazo, Facultad de Mecánica, Investigation Group GIEBI; [edwin.pozo@esPOCH.edu.ec](mailto:edwin.pozo@esPOCH.edu.ec), ORCID: 0000-0002-9658-6311
- <sup>6</sup> Investigador independiente, Riobamba, Ecuador; [santiagoChoto@gmail.com](mailto:santiagoChoto@gmail.com), ORCID: 0000-0003-0655-2503

\* Correspondence: [lidia.castro@esPOCH.edu.ec](mailto:lidia.castro@esPOCH.edu.ec)

**Abstract:** This research work allows us to determine the behavior of concrete as an acoustic inhibitor, for this we start from a deep bibliographical search related to the propagation of sound and its properties, focused on hollow blocks whose material is concrete. The experimental tests are based on the NTE INEN standard where the transmission losses in the sound propagation are analyzed together with the properties of said material, under the same standard the tests are carried out in the experimental part and the necessary calculations of the different parameters, data that will later be used in the simulations. To carry out the simulations, the COMSOL Multiphysics software is used, with the *poracoustic* domain function that uses the Johnson-Champoux-Allard mathematical model, which allows characterizing the acoustic properties of the analyzed concrete in terms of the angle of incidence of the wave from 0° to 45° and frequency. For the validation of the model, the values of the simulated acoustic absorption coefficient and the impedance of the surface are considered with the analytical results. Finally, with this study, the acoustic behavior of concrete in the form of hollow blocks is identified and the values of the acoustic absorption coefficient are obtained through simulations and experimental design.

**Keywords:** acoustic absorption, simulation, noise, concrete, mathematical modelling.

## 1. Introduction

In recent years, noise pollution has become a major international problem. Studies conducted in Europe indicate that the world is currently facing problems with so-called ambient noise, as all kinds of activities, especially in the economic, social, and industrial realms, contribute to increasing noise pollution [1]. Worldwide, it is recorded that noise in populated cities exceeds 65 dB(A) [2], According to the Organization for Economic Co-operation and Development (OECD) [3], at least 130 million people are exposed to noise levels that exceed this value during the day, and a large part of them suffer from noise pollution above the limits established by the World Health Organization (WHO) [4]. It is also stated that noise in quantity is expended by the amount of sound generated by everyone in a short or spacious period [2].

According to reports issued by the Health and Environment Observatory, around 30% of the population in Spain, more than 9.5 million people, live with noise levels that exceed the levels considered adequate for human health. And nearly 20 million could be subject to lower levels, but which can also cause health problems if exposed for long periods of time. It is estimated that due to noise, Europeans lose 1.6 million years of healthy life every year, a calculation combining the potential years of life lost due to premature deaths and the equivalent years of healthy life not enjoyed due to deteriorating health [5].

For this reason, researchers have shown interest and spoken out through scientific publications in the academic community that the level of noise pollution in recent years is extremely high, becoming one of the most relevant problems in the world. This is due to technological advances that have allowed society to evolve, but at the same time have generated new threats to health. While noise does not tend to accumulate like other pollutants, it could cause long-term hearing problems if not controlled, making it difficult to maintain a relaxed and healthy lifestyle. Therefore, any solution to noise will help improve the physical and mental environment [6].

From this bibliographic analysis, there is a need to provide constructive solutions that protect individuals from acoustic shocks, directly improving their quality of life and hearing health standards [7]. Construction materials have different properties that characterize them and are useful for their selection, considering their shape, resistance, hardness, versatility, and size. Leaving aside important properties for certain constructions, one of them is acoustic absorption, which uses materials that reduce the energy of reflections, making them less harmful, thus avoiding sound focalizations.

This research is based on the analysis of one of the main parameters of acoustic behavior: the absorption coefficient in hollow concrete blocks and its behavior as an acoustic inhibitor, through simulations. Since at the start of a construction project, the acoustic and absorbing properties of one material over another are not considered, which could allow for control of noise pollution caused by excessive ambient noise, the cost of construction materials and the tradition in their use

become important. This research focuses on the need to evaluate acoustic behavior through the simulation of commonly used concrete blocks as construction elements, allowing for the determination of the absorption coefficient, an important parameter to consider a material as an acoustic inhibitor. To do this, some parameters are considered, such as noise levels that can exceed 80 dB in industries and adjoining residential areas for periods of exposure greater than one hour, considering that the maximum permissible limit is 70 dB in industrial areas, generating polluted spaces for the population [8].

The research has three phases: the first is focused on analyzing the problem; the second is an exhaustive literature review that allows for the generation of research antecedents; a third phase includes obtaining results and discussion, and finally, drawing conclusions. To quantify sound levels, the fundamental parameters of analysis considered are sound pressure, intensity, and frequency, which can determine if a sound is strong or weak using some physical quantities that help describe the sound phenomenon. Regarding simulation, the Finite Element Method (FEM) has been selected, using the poroacoustic domain function based on the Johnson-Champoux-Allard mathematical model, which will be used in the software solver. With these arguments, it is possible to define the characteristics of concrete acting as an acoustic inhibitor that can be used in constructions exposed to high concentrations of noise, achieving structurally secure environments, and reducing noise pollution.

### ***1.1 Simulation and behavior of sound waves in building materials.***

Researchers have seen the need to improve the acoustic properties of building materials to create spaces that guarantee better living conditions in areas exposed to high levels of acoustic noise. According to Fiala, the starting point for improving these materials lies in identifying their acoustic properties and modeling them based on a mathematical requirement of exposure acoustic loads. Fiala also considers that a material's attenuation depends on its porosity and volume. Additionally, the geometry of the pores can be filled with some type of additive (bulk materials) to help improve the dispersion and attenuation of acoustic waves [9].

Concrete is one of the most common and widely used materials at all levels of construction. According to Fediuk, its design is important in a building, but it is mandatory to consider the structural parameters and acoustic properties it must have. These properties allow for comfortable living spaces and improve people's comfort conditions. Different concrete compositions behave differently as sound conductors, with dense mixes acting as sound reflectors and lightweight mixes acting as absorbers. The type of reflection that concrete can have depends on the aggregates and changes in the design components of the mix. Therefore, the acoustic absorption of concrete with acoustic insulation (AIC) can be improved by changing its configuration, adding a porous element or a foam agent [11].

Pereira presents a new concept of acoustic absorption called meta-porous concrete, which is a sound absorber consisting of porous concrete containing different acoustic resonators. For this study, two finite element models were implemented using equivalent fluid theory to describe the solutions of meta-porous concrete. With the help of a Helmholtz resonator, samples of porous concrete and concrete test specimens are experimentally tested through the impedance tube technique, allowing for finding the properties of the equivalent fluid and validating the properties with analytical predictions and experimental data. It is worth mentioning that the proposed numerical models and methodology allow predicting acoustic absorption in meta-porous concrete, considering the simulated results and experimental data. The experiment, given the inclusion of resonant structures in porous concrete, allows building a meta-porous concrete that can be used in controlling noise in outdoor civil constructions [12].

## 1.2 *Wave behavior as acoustic inhibitors*

There are several strategies implemented to solve problems of acoustic resonance, from methods such as placing absorbing elements in the corners of rooms, to the design of Helmholtz resonators, where the management of frequency bands allows the efficiency or not of each method [13]. Recent research analyzes this problem in depth, indicating that the acoustic absorption found in perforated ceramic panels is based on the principle of Helmholtz resonators, considering that this method is efficient with narrow frequency bands; for the absorption phenomenon to be effective, the ceramic panels are perforated and mounted on a rigid surface. [14].

As part of the procedure for measuring the coefficient of normal incidence sound absorption, an impedance tube or Kundt tube with an internal diameter of 10 cm and a length of 56 cm is used. The valid measurement range for the coefficient of sound absorption is from 100 Hz to 2 kHz.

Several investigations have found that the attenuation zones that have different frequencies are one of the main problems in the field of materials. In this case, they analyzed the flexural waves and the properties of the attenuation zone of periodically perforated plates with cross-shaped holes, using the finite element software ANSYS, to obtain dispersion curves for flexion. The results showed that plates with cross-shaped perforations can generate lower and multiple attenuation zones compared to those with other geometric configurations, such as squares and diamond-shaped holes [15].

The acoustic behavior of the samples is analyzed using a numerical method, and the development of a code to simulate the structure in 3D and the calculation of tortuosity and two characteristic lengths in a numerical software. The Johnson-Champoux-Allard (JCA) model is used to predict the SAC at different frequencies. As a result, the acoustic behavior of the optimized acoustic panels in the reverberation room is in terms of reverberation time and random absorption coefficient [16].

### ***1.3 Numerical simulation methods for wave propagation.***

In current research, mathematical models are used to characterize the sound field and schematize the impulse response of the enclosure, making it a valuable tool for acoustic design and analysis. Cravero, in his study, presents results of measurements of reverberation time and acoustic properties in classrooms using the integrated response method according to IRAM 4109-2. The next step is to compare the measured values with those simulated using computational calculation tools. Finally, in the analysis of results, the measurements are compared with the recommendation given in the ANSI S12.60 standard and international bibliographic references [17]. Another mathematical model for the vibro-acoustic analysis of a 17-story structure shows good correlation with the measured data. It should be noted that the selection of a numerical method depends on the frequency domain. For a low-frequency domain, the finite element method (FEM) or the boundary element method (BEM) is preferred. FEM is considered for computational simulations, as the research is limited to low-frequency regions [18].

One of the most used numerical methods for porosity and absorber analysis is the Johnson-Champoux-Allard-Lafarge (JCAL) model, applied to calculate the five transport parameters of the JCAL model, including viscous permeability, thermal permeability, tortuosity, viscous characteristic length, and thermal characteristic length. These values allow modeling of the rough tubes in porous materials, such as parallel rough tubes with idealized sinusoidal morphologies. Finally, the results have shown that the presence of roughness in the tubes weakens the thermal effect, but drastically reinforces the viscous effect in dissipating sound energy, resulting in improved sound absorption [19].

## **2. Materials and Methods**

### **2.1 Equipment and materials**

#### **2.1.1 Hollow concrete blocks**

The standard used for the manufacture of hollow concrete blocks is: Hollow Concrete Blocks. Definitions, Classifications and Conditions. Table 1 indicates the types of hollow blocks available in the market and their dimensions. For this study, the type B concrete block has been selected [20].

**Table 1.** Types of hollow concrete blocks and their uses.

NOMINAL DIMENSIONS				ACTUAL DIMENSIONS			USES
Block type	length	width	height	length	width	height	
A, B	40	20	20	39	19	19	<ul style="list-style-type: none"> <li>○ External load-bearing walls, without coating.</li> <li>○ Exterior load-bearing walls, with cladding.</li> <li>○ Interior load-bearing walls, with or without lining.</li> </ul>
		15			14		
		10			09		
C, D	40	10	20	39	09	19	<ul style="list-style-type: none"> <li>○ Exterior dividing walls without cladding,</li> <li>○ Exterior dividing walls, with cladding.</li> <li>○ Interior dividing walls, with or without lining.</li> </ul>
		15			14		
		20			19		
E	40	10	20	39	09	20	<ul style="list-style-type: none"> <li>○ Lightened reinforced concrete slabs.</li> </ul>
		15			14		
		20			19		
		25			24		

Standar NTE-INEN [21] [20]

The dimensions of the block to be used are as follows: length = 40 cm, width = 15 cm, height = 19 cm, and an approximate weight of 8.5 kg as shown in Figure 1. The regulation states that the blocks must have uniform dimensions, although the variation in their lengths should not exceed 5 mm. [20].

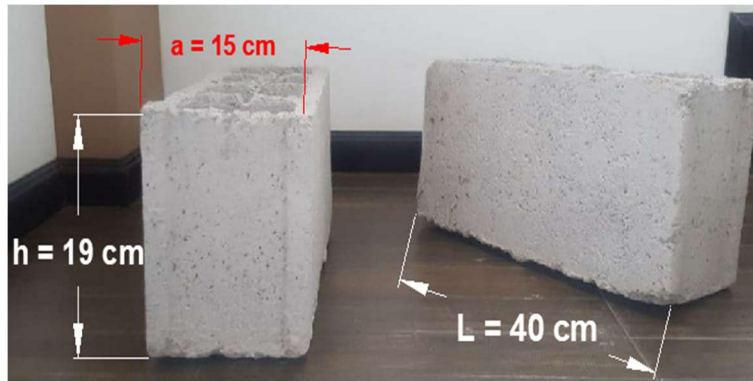


Figure 1. Lengths of concrete hollow block samples.

### 2.1.2 Standards for conducting tests.

Table 2 details the standards to be applied in the experimental phase, for carrying out tests such as density, porosity, and mechanical strength in the concrete bricks and blocks, parameters necessary for carrying out acoustic simulations.

Table 2. NTE INEN standards used to carry out the tests.

Test	Standard used	Parameters
Density	<ul style="list-style-type: none"> <li>Refractory Materials. Determination Of Porosity, Water Absorption and Bulk Density. NTE INEN 857:2010.</li> <li>Concrete blocks. Requirements and test methods. NTE INEN 3066-2016</li> </ul>	Specimens' density
Porosity	<ul style="list-style-type: none"> <li>Refractory Materials. Determination Of Porosity, Water Absorption and Bulk Density. NTE INEN 573.</li> <li>Concrete blocks. Requirements and test methods. NTE INEN 3066-2016</li> </ul>	Total Porosity Percentage
Mechanical strength	<ul style="list-style-type: none"> <li>Ceramic bricks. Part 5: Test Methods. NTE INEN 3049 Part 5:2019.</li> <li>Concrete hollow blocks, related units, and prisms for masonry. Facing for the compression test. NTE INEN 2619:2012</li> </ul>	Stress

Standard NTE INEN [22][23] , [24][25], [26][27], [28][29], [30]

### 2.1.3 Software COMSOL Multiphysics

COMSOL Multiphysics is an efficient simulation software used to model and solve scientific and engineering problems. This software uses FEM and partial differential equations. Being a powerful

simulation tool, it allows combining conventional physics models into Multiphysics models that can be solved simultaneously. With an integrated desktop environment and Model Builder, the user can fully describe the model and access all the necessary functions for its use. The interface can be seen in Figure 2.

The advantages of COMSOL Multiphysics lie in the possibility of integrating physical parameters, material properties, loads, constraints, sources, etc., instead of defining equations, which are found in the different modules presented by the program. The variables of the mathematical model can be placed directly into the software, such as domains, limits, edges, and solid and fluid points, independently of the computational mesh. Ultimately, the package compiles the equations that govern the model internally [31][32].

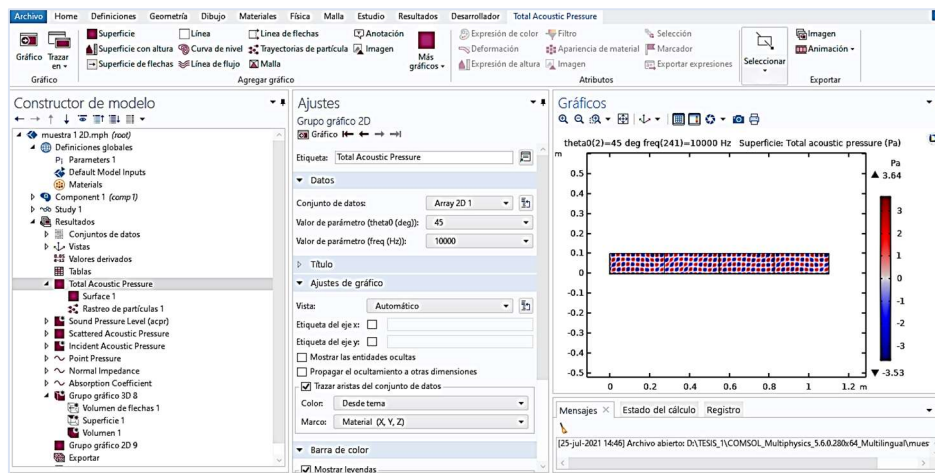


Figure 2. COMSOL Multiphysics interface [33] [31]

The COMSOL Multiphysics software then internally compiles a set of equations that represent the complete model. By using advanced numerical analysis tools, it also analyzes the mesh created for the case and, based on the numerical solvers it has, presents acceptable errors within established ranges. The software allows for visualization and presentation of the results.

### 2.1.4 Calculation of Young's Modulus

The modulus of elasticity is the ratio of stress increment to the corresponding unit strain change. If the stress considered is either tension or compression, the modulus is called Young's modulus [34]. For the analyzed hollow concrete blocks, compression tests were carried out, where data on the last applied stress and deformation were collected. Equation 1 allows for the calculation:

$E = \frac{\sigma}{\epsilon}$	Equation 1
-------------------------------	------------



Where,  $E$  represents the Young's Modulus,  $\sigma$  is the uniaxial stress or force per unit area, and  $\epsilon$  is the strain. The value of strain ( $\epsilon$ ) is shown in Equation 2, where  $\Delta L$  is the change in length and  $L$  is the initial length:

$\epsilon = \frac{\Delta L}{L}$	Equation 2
---------------------------------	------------

### 2.1.5 Sound velocity

The speed of sound is that which propagates through a material medium, such as air, water, or a solid, by means of a sound wave. The speed of sound depends on the properties of the medium through which it propagates and the temperature of that medium. At room temperature, the speed of sound in air is approximately 343 meters per second (m/s). The expression used in the analysis of concrete samples is a function of the Young's Modulus  $E$  and the density  $\rho$ , resulting in Equation 3 .

$v_s = \sqrt{\frac{E}{\rho}}$	Equation 3
-------------------------------	------------

### 2.1.6 Sound pressure level

The sound pressure level (SPL) is a measure of the amount of energy associated with noise, caused by a disturbance of a medium due to the vibration of a bod [35]. Sound pressure is measured in Pascals (Pa) and a logarithmic scale is commonly used for its manipulation and representation due to the large range of values it can present. The reference pressure used in Equation 4 is the human auditory threshold, which has been established at a value of  $2 \times 10^{-5} Pa$  by convention. It is important to mention that SPL values can vary widely depending on the sound source and the location of the observer.

$L_p = 20 \log \left( \frac{P}{P_0} \right)$	Equation 4
--	------------

### 2.1.7 Reflection

For the study of acoustic reflection, two different zones must be considered. The first is called the zone of first reflections, which arrive immediately after the sound emission. The second is called the reverberant tail, formed by delayed reflections. It is necessary to represent this zone, observing how the incident rays arrive and the energy level generated [36].

### 2.1.8 Acoustic impedance

Acoustic impedance is a property that provides information about the medium and the type of wave that will propagate. This calculation, of great importance, involves the transmission of acoustic waves from one medium to another [37]. The following expression allows the calculation

of acoustic impedance ( $Z$ ), where  $p$  is the acoustic pressure and  $v$  is the velocity associated with the oscillating particles in a medium.

$Z = \frac{p}{v}$	Equation 5
-------------------	------------

### 2.1.9 Calculation of the absorption coefficient in COMSOL Multiphysics.

The acoustic absorption coefficient refers to the ability that all materials have to mitigate the propagation of sound waves when they impinge on them. Therefore, octaves should be considered, since the human ear hears logarithmically, and frequencies are divided in this way, this is known as octaves, [38], where an octave is defined as the interval that separates one frequency from another by a factor of two. According to the NTE INEN 266 standard [39], Table 3 indicates the most used octave bands in Hz.

**Table 3.** Most used octave bands in Hz.

Octave Band Center Frequencies										
16	31.5	63	125	250	500	1000	2000	4000	8000	16000

Standar NTE INEN 266 [39]

In this research, the property will be calculated through simulations of acoustic behavior in COMSOL Multiphysics software, and it has been considered that for greater accuracy and resolution of the phenomenon, the developed frequency will be given in third-octave bands. For this purpose, the Porous Absorber has been taken as a reference model, one of the models based on the Acoustic Poro domain of the acoustic pressure interface, described in the User's Guide of the Acoustics Module [40], which uses the Johnson-Champoux-Allard model as a numerical solver for the characterization of absorption properties of a common brick in terms of sound incidence angle and frequency [41].

In general, this model analyzes Johnson-Champoux-Allard (JCA) porous matrices, which are defined by the equivalent rigid density  $\rho_{rig}(\omega)$  and the equivalent volumetric modulus  $K\omega$ . The mathematical expressions for these parameters are described below,[40]:

$\rho_{rig} = \frac{\tau_{\infty} \rho_f}{\epsilon_p} \left[ 1 + \frac{R_f \epsilon_p}{i \omega \rho_f \tau_{\infty}} \sqrt{1 + \frac{4 \omega \tau_{\infty}^2 \mu \rho_f}{R_f^2 L_v^2 \epsilon_p^2}} \right]$	Equation 6
--	------------

$K = \frac{\gamma P_A}{\epsilon_p} \left[ \gamma - (\gamma - 1) \left( 1 + \frac{8\mu}{i\omega L_{th}^2 Pr \rho_f} \sqrt{1 + \frac{i\omega L_{th}^2 Pr \rho_f}{16\mu}} \right)^{-1} \right]^{-1}$	Equation 7
---	------------

Where:

$\tau_\infty$  = tortuosity factor (high-frequency limit),  $\rho_f$  = fluid density,  $\epsilon_p$  = porosity,  $R_f$  = flow resistivity,  $\mu$  = dynamic viscosity,  $p_A$  = inactive pressure,  $\gamma$  = specific heat ratio,  $L_v$  = viscous characteristic length,  $L_{th}$  = thermal characteristic,  $Pr$  = Prandtl number.

### 2.1.10 Tests for calculating block properties.

The tests carried out will allow obtaining data through experimentation that will validate the found parameters, to finally evaluate their behavior through the execution of simulations in specialized software. The tests carried out are described below:

#### - *Density and Absorption of the block*

This test is carried out under the NTE INEN 3066:2016-11 [29], Standard, Concrete Blocks. Requirements and Test Methods, Absorption, Density, and others. This allows determining the density of the samples, the necessary steps for its execution are described below, [28]:

- Three complete samples without defects must be considered for the tests.
- A balance with an accuracy of  $\pm 1$  g of mass will be needed.

For the saturation procedure, the samples must be immersed at a temperature between 16°C and 27°C for a time of 24 to 28 hours in a container that completely covers them and record this value as M<sub>I</sub> (mass of the immersed sample), as shown in Figure 3.

Next, remove the samples from the water and let them drain for 60 s on a metal mesh, and dry them with a damp cloth, determine the mass, and record it. Repeat the procedure every 24 hours until the weighing difference is less than 0.2%. Record the result as M<sub>S</sub> (mass of the saturated sample).

Dry the samples in a ventilated oven, between 100 °C and 115 °C, take weight measurements every 24 hours until the weight difference is less than 0.2%. Record this value as M<sub>d</sub> (Mass of the oven-dried sample).



Figure 3. Samples of blocks submerged in water for density and absorption percentage calculation.

The equations for calculating density and absorption according to standard [28] for concrete blocks are detailed below:

<b>Absorption:</b>	
$Absorption = \frac{M_s - M_d}{M_s - M_i} \times 1000 \left[ \frac{kg}{m^3} \right]$	Equation 8
$Absorption = \frac{M_s - M_d}{M_d} \times 100 \text{ [%]}$	Equation 9
<b>Density:</b>	
$Densidad = \frac{M_d}{M_s - M_i} \times 1000 \left[ \frac{kg}{m^3} \right]$	Equation 10

Where,  $M_s$  is the mass of the saturated unit,  $M_i$  is the mass of the immersed unit,  $M_d$  is the mass of the unit dried in the oven, with units given in [kg].

- **Mechanical strength tests: Compression test for hollow concrete blocks.**

To carry out this test, the recommendations of standard NTE INEN 640, Hollow Concrete Blocks. Determination of compressive strength, which indicates the following steps, [42]:

- Use whole blocks selected according to standard INEN 639 [29].
- The blocks must be immersed in water for a period of 24 hours and then covered with cement-sand mortar with a layer no more than 6 mm thick, so that the tested surfaces are regular and parallel.

To test the samples, they must be placed with respect to the center of the load application joint. The load application will be gradual, in a time not less than 1 minute or greater than two, considering a constant speed, Figure 4.

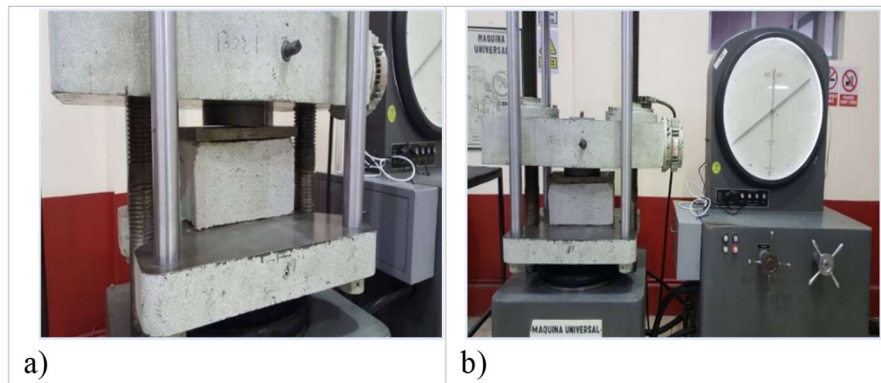


Figure 4. (a) Complete specimens (hollow concrete blocks) (b) Compression test on a universal testing machine.

- **Simulation of acoustic behavior in COMSOL Multiphysics V. 5.6, of the block samples (B1, B2).**

To carry out the simulations, the absorption model through an open-cell porous acoustic foam (Porous Absorber) was taken as reference, from which modeling instructions are described [42].

- **Response variables or achieved results.**

To achieve the objectives, the transmission of sound waves on existing construction materials is considered as an independent variable. This is because each of them has acoustic properties that absorb, transmit or reflect sound when waves impact on them. The dependent variable is the behavior of the materials as acoustic inhibitors, that is, the property of material absorption that manifests as incident energy dissipated upon contact with a material, affecting sound propagation.

As a result, the value of the acoustic absorption coefficient is desired through the execution of simulations in the COMSOL Multiphysics software, characterizing the absorption properties of hollow concrete blocks in terms of sound incidence angle and frequency. The model results will be validated by comparing them with analytical data to indicate if traditional brick and hollow concrete block meet the requirements to be considered as acoustic inhibitors.

### 3. Results

#### 3.1 Test Results

##### 3.1.1 Concrete hollow blocks

Concrete hollow blocks are widely used in construction due to their great maneuverability. Those selected for this study follow the following construction standard [21]. Hollow Concrete Blocks.

Definitions, Classifications and Conditions. The dimensions and type of block used in the tests and simulations are shown in Table 4.

**Table 4.** Type and dimensions of concrete hollow blocks in cm.

NOMINAL DIMENSIONS				ACTUAL DIMENSIONS	
Block Type	Long	Width	High	Long	Width
A, B	40	20,15,10	20	39	19,14,09

Standard NTE INEN [21]

For the calculation of density in the block samples, the NTE INEN 3066-2016 standard, Concrete Blocks. Requirements and Test Methods, Annex D (normative) Absorption, Density, and others, is considered. The results are shown in Table 5.

**Table 5.** Density values of hollow concrete block samples.

Specimen	Masses [kg]			Density [kg/m <sup>3</sup> ]
	Saturated unit mass [Ms]	Oven-dry unit mass [Md]	Submerged unit mass [Mi]	
B1	10.05	8.21	10.01	205205
B2	10.00	8.43	9.96	210750

### 3.1.2 Test for porosity

For the calculation of absorption, the NTE INEN 3066-2016 standard, Concrete Blocks - Requirements and Test Methods, Annex D (normative) Absorption, Density, and others, is considered. The results are shown in Table 6.

**Table 6.** Total absorption values [%]

Specimen	Masses [kg]			Absorption [%]
	Saturated unit mass [Ms]	Oven-dry unit mass [Md]	Submerged unit mass [Mi]	
B1	10.05	8.21	10.01	22.41
B2	10.00	8.43	9.96	18.62

### 3.1.3 Mechanical strength tests.

For hollow concrete blocks, the recommended mechanical strength test is given by the standard NTE INEN 2619:2012 Hollow Concrete Blocks, Related Units and Masonry Prisms. Refacing for compression testing. Table 7 shows the results obtained in the compression test on the blocks.

**Table 7.** Compression test results (stress and strain)

Samples	Test tube	Stress ( $\sigma$ )	Strain
		[N/m <sup>2</sup> ]	[mm]
B1	1	225356.22	2.33
	2	174451.25	1.39
	3	157371.48	1.63
<b>Mean</b>		<b>185726.31</b>	<b>1.78</b>
B2	1	226371.64	1.08
	2	197663.65	1.62
	3	166402.81	1.55
<b>Mean</b>		<b>196812.70</b>	<b>1.42</b>

The values obtained for Young's modulus and sound velocity for the hollow concrete blocks are shown in Table 8. These parameters are necessary for performing simulations.

**Table 8.** Young's modulus and sound velocity values.

Specimen	Módulo de Young	Velocidad sonido (c)
	[Pa]	[m/s]
B1	104145.59	0.71
B2	138926.61	0.81

### 3.1.4 Results of COMSOL Multiphysics simulation to obtain the acoustic absorption coefficient ( $\alpha$ )

These results are obtained by performing simulations of samples in hollow concrete blocks (B1 and B2) using the previously described procedure. It is important to mention that the simulation was carried out considering a frequency range from 10 Hz to 10 kHz, with a 1/3 octave step and an angular incidence of the wave from  $0^\circ$  to  $45^\circ$ . These parameters entered the software result in graphs of Sound Pressure vs Frequency, Impedance vs Frequency, and Absorption Coefficient vs Frequency. These are the results of 2D simulations applied to the main face of the block, where the sound wave directly impacts. Additionally, 3D simulations are performed to verify the incidence of the acoustic wave on the building material, and the resulting graphs are:

- **Results of 2D and 3D simulations of hollow concrete block samples B1 and B2**

***Simulations of sample block B1 in 3D***

The 3D simulation of the hollow concrete block sample B1 is shown in Figure 5, where the incidence of the wave at  $45^\circ$ , with a frequency of 99.986 Hz, results in maximum values of acoustic pressure (in red) from 2 to 4 [Pa]. Note that these pressure concentration values occur on the faces of the block where there is greater acoustic incidence. In addition, the studied body is shown in the YZ plane, which allows for a better identification of the incidence of the sound pressure on the simulated sample.

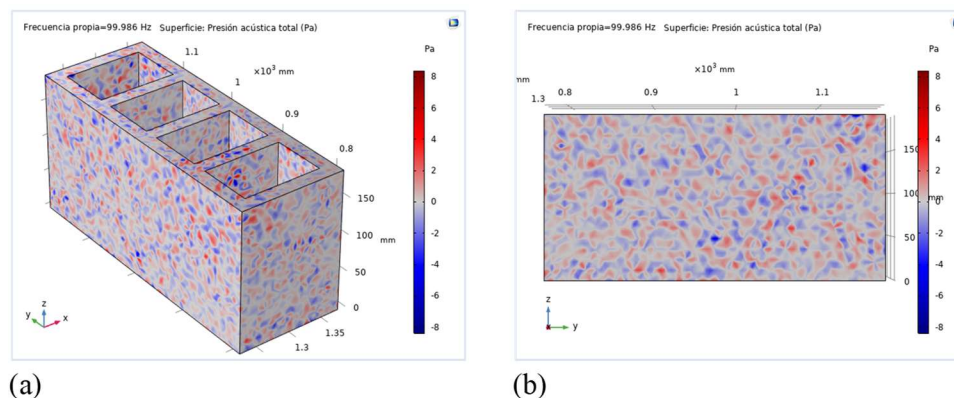


Figure 5. (a) Simulation of Sample B1. (b) Show B1 in the YZ plane.

The distribution of sound pressure level over sample B1 is shown in Figure 6, a result of the 3D simulation where the eigenfrequency with a value of 99.989 Hz impinges on the faces of sample B1, generating sound pressure level values over the block's hollows between 90 to 100 dB. It's worth noting yellow areas throughout the simulated sample with an approximate value of 70 dB. These values can vary mainly due to the incident sound speed on the material. The yellow area of the sample can be better observed in the XZ plane.



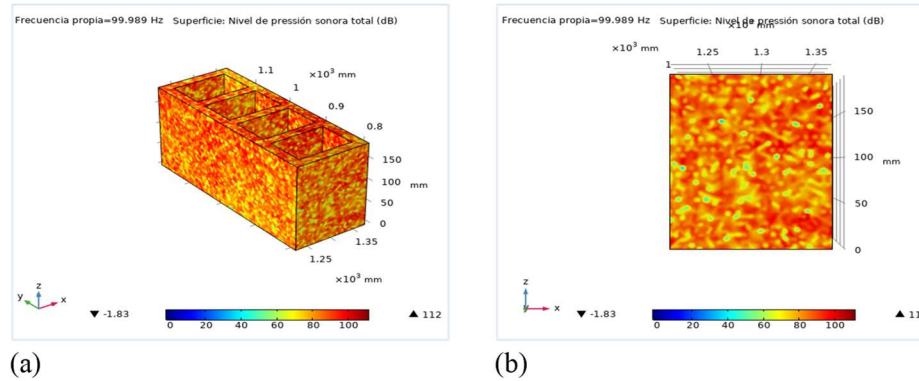


Figure 6. (a) Distribution of the sound pressure level on sample B1. (b) Distribution of sound pressure level in the XZ plane.

To obtain better results of sound pressure level in the simulation of sample B1, the mesh is refined with a natural frequency value of 99.996 Hz. As can be seen in the color bar in Table 7, these values range between 85 to 100 dB, and a different pattern of the incidence of the acoustic wave on the block can be seen. These images have been produced mainly due to the number of elements in the mesh after refinement, aiding in the convergence of the simulation.

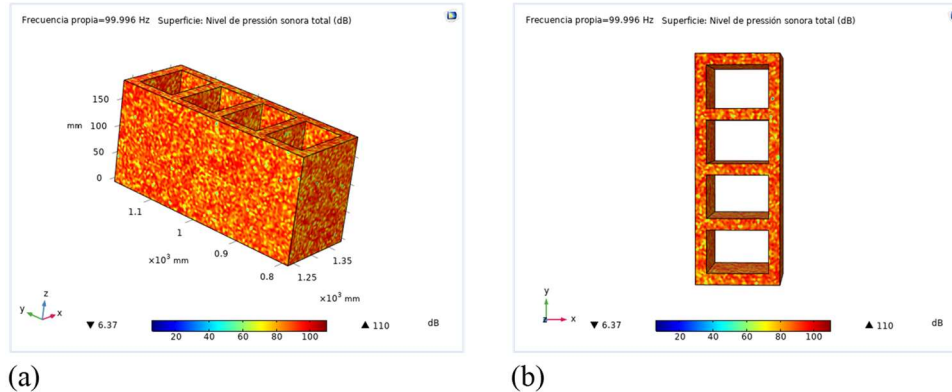


Figure 7. (a) Simulation of Sample B1 with refined mesh. (b) Sample B1 in the XY plane with mesh refinement.

## - 2D Simulations

The simulated B1 sample in 2D allows the following results:

### Sound pressure vs Frequency

Figure 8 shows the sound pressure as a function of frequency [Hz] and total acoustic pressure [Pa] considering the incidence of the wave, for which two incident angles ( $\theta$ ) = 0° and ( $\theta$ ) = 45° have been analyzed. The incident angle (AI) ( $\theta$ ) = 45° presents an irregular behavior compared to the curve that describes the incident angle (AI) ( $\theta$ ) = 0°, and as a result, a maximum value of 4.83 [Pa] of total acoustic pressure is obtained with a frequency of 250 Hz. These values are within the range

that the human ear perceives and tolerates, ranging from 20 to 20,000 Hz. The simulation has demonstrated that the block functions as a sound inhibitor.

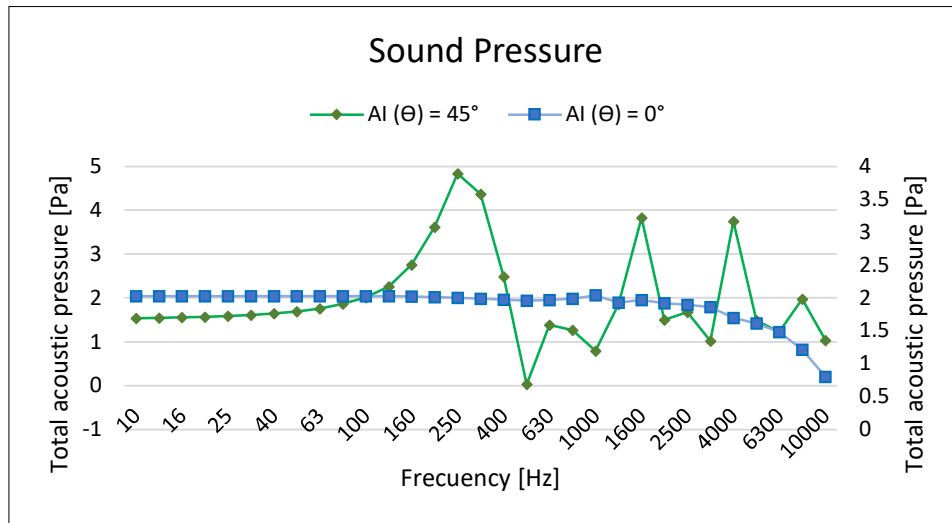


Figure 8. Total acoustic pressure vs Frequency in sample B1.

**Impedance vs Frequency**

As impedance is an important property that relates acoustic pressure and the velocity at which oscillating particles develop in a medium, at a given frequency, Figure 9 allows identifying these values, considering the wave generated by the incidence angle (θ) = 45°. Specific surface normal impedance (black curve) can be observed to decrease as frequency increases. A value of  $Z = 21.63$  (dimensionless) is obtained at a frequency of 10 Hz, which remains stable until a value of  $Z = 21.05$  at a frequency of 40 Hz. Thus, it can be concluded that the velocity of particles will decrease as frequency increases.

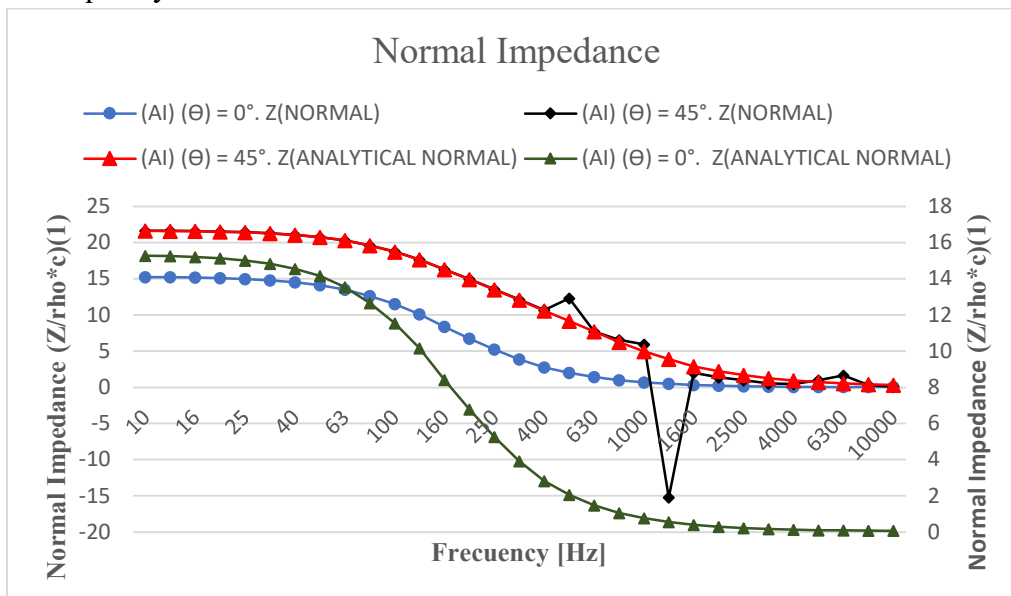


Figure 9. Normal impedance of sample B1 with different angles of incidence

**Absorption coefficient vs Frequency**

Figure 10 shows the results of the 2D simulation for the absorption coefficient  $[\alpha]$  of sample B1, where the values of the coefficient on the curve can be identified for the absorption coefficient with incidence at  $45^\circ$  ((AI)  $(\Theta) = 45^\circ \alpha$ ), with a maximum value of  $\alpha = 0.97$ ,  $f = 1.0$  kHz, and  $\alpha = 0.29$ ,  $f = 10$  kHz, which corresponds to the linearization of the incidence angle at  $45^\circ$  (analytical curve for the absorption coefficient with incidence at  $45^\circ$  (AI)  $(\Theta) = 45^\circ$ . ( $\alpha$  analytical)). This difference between these values is due to the irregularity of the curve at  $45^\circ$  from 630 Hz, as well as the value of the speed of sound and the density of the material, which are properties of great importance in simulations.

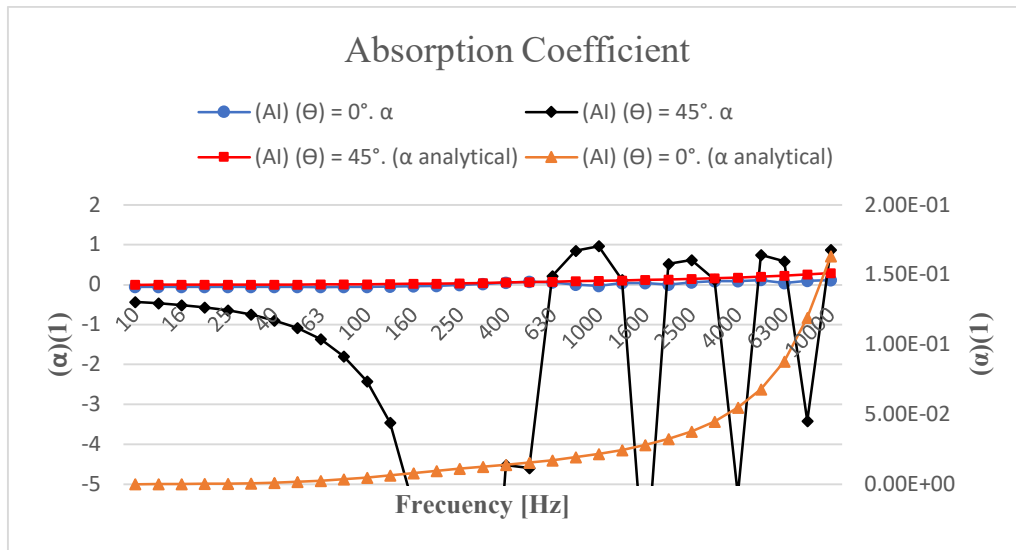


Figure 10. Absorption coefficient vs Frequency with the different angles of incidence

**3D block B2 sample simulations**

Figure 11 shows the 3D simulation result of the second sample of the hollow concrete block (B2), where the incidence of the wave at  $45^\circ$  with a frequency of 99.987 Hz can be observed. Variations in pressure can be seen that produce areas of higher particle concentration (areas of red color) on

different faces of the building material, with values ranging from 2 to 6 [Pa]. In addition, the XZ plane has been considered for the study, which allows for a better identification of the incidence of sound pressure on the simulated sample.

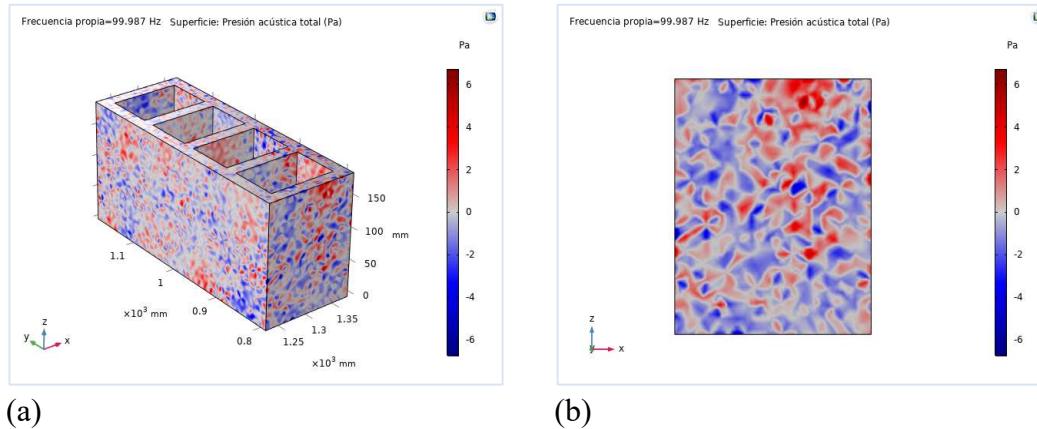


Figure 11. (a) Simulation of Sample B2. (b) Show M2 in the YZ plane.

The distribution of sound pressure level over sample B2 is shown in

Figure 12, which is the result of the 3D simulation where the natural frequency of 99.991 Hz impinges on the faces of the block, generating sound pressure level values between 90 to 100 dB (areas of concentration of red color). It is important to mention the yellow areas present throughout the block that repeat simultaneously with time (frequency) with an approximate value of 70 dB. The yellow area of the sample can be better observed in the XZ plane.

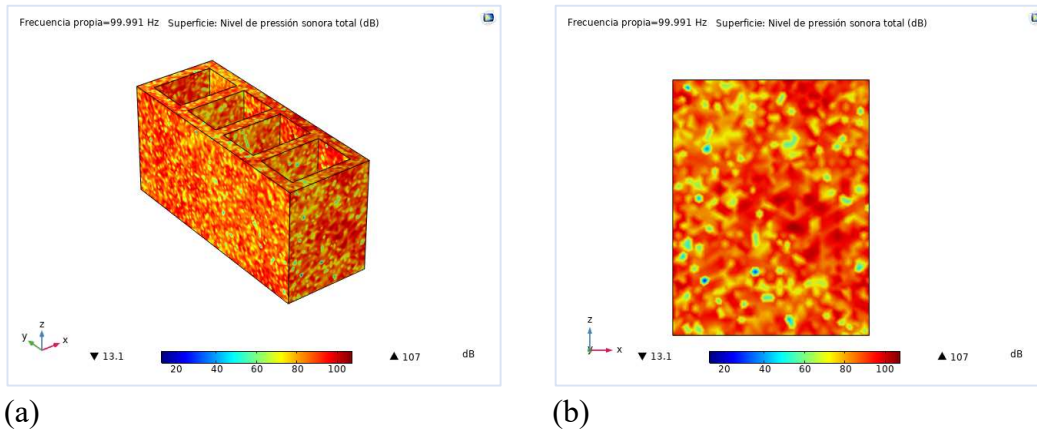


Figure 12. (a) Distribution of the sound pressure level on sample B2. (b) Distribution of sound pressure level in the XZ plane.

The mesh refinement allows us to observe the results of sound pressure level in the simulation of sample B2, with a natural frequency value of 99.995 Hz. The maximum concentration values are between 90 to 100 dB, which are shown in the color bar. Additionally, in Figure 13, a different plot of the incidence of the acoustic wave on the block can be seen, which depends on the value of the speed of sound, which for this sample is 0.81 m/s. It should be mentioned that these images were mainly produced by the number of elements in the mesh after refinement.

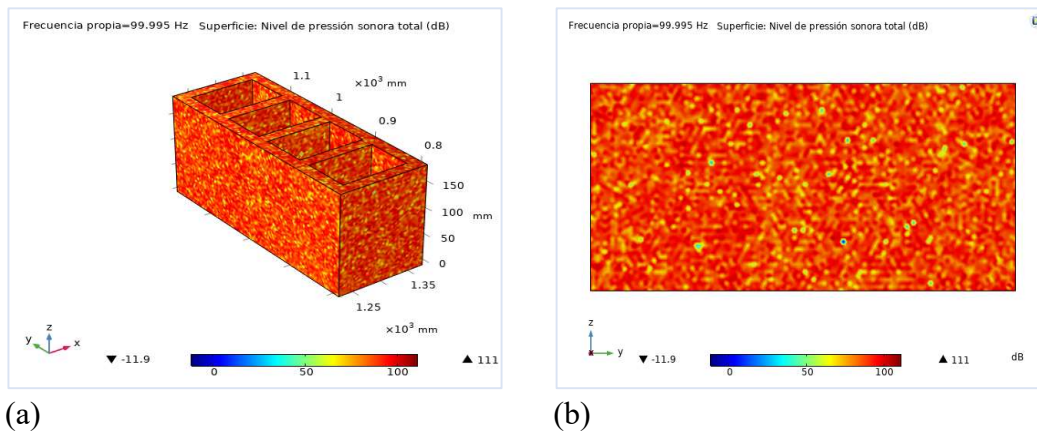


Figure 13. a) Results of the sound pressure level in the simulation of sample B2 with refined mesh. (b) Sample B2 in the XZ plane with mesh refinement.

### Simulations in 2D

#### Sound Pressure vs Frequency

Figure 14 shows the sound pressure considering two incident angles  $(\Theta) = 0^\circ$  and  $(\Theta) = 45^\circ$ . The incident angle (AI)  $(\Theta) = 45^\circ$  (green curve) presents an irregular behavior compared to the curve that describes the incident angle (AI)  $(\Theta) = 0^\circ$ . In addition, the maximum total acoustic pressure

value obtained is 4.861 [Pa] at a frequency of 250 Hz. These values will vary depending on the speed of sound.

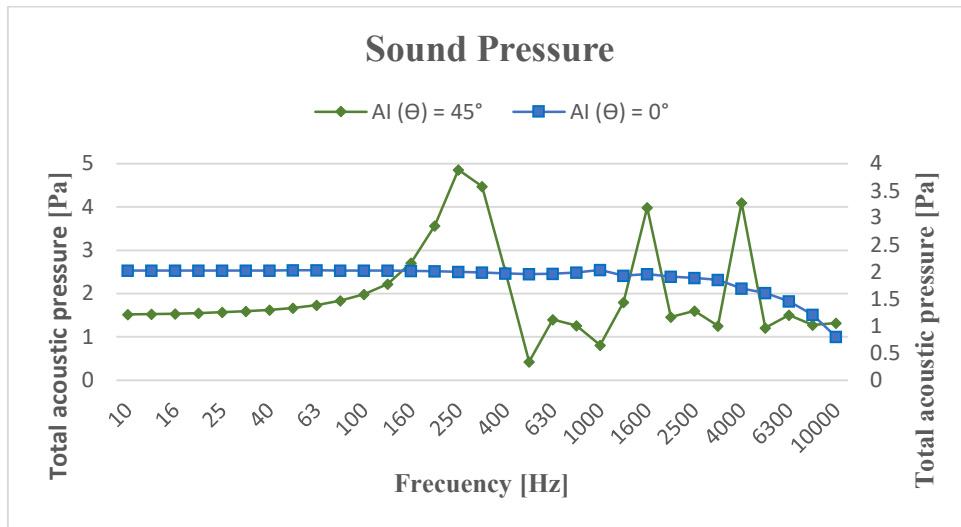


Figure 14. Total acoustic pressure vs Frequency in sample B2.

### Impedance vs Frequency

Figure 15 shows the values of impedance, a property that relates acoustic pressure, velocity, and the frequency with which oscillating particles develop in a medium. The wave generated by the angle of incidence ( $\Theta$ ) = 45° has been considered. Specific surface normal impedance (black curve) is shown, where it can be observed that impedance decreases as frequency increases. A value of  $Z = 21.63$  (dimensionless) is obtained at a frequency of 10 Hz, and this value remains stable until a value of  $Z = 21.07$  is reached at a frequency of 40 Hz. Therefore, it can be determined that the velocity of the particles that develop on a medium is a determining factor in the value of impedance.

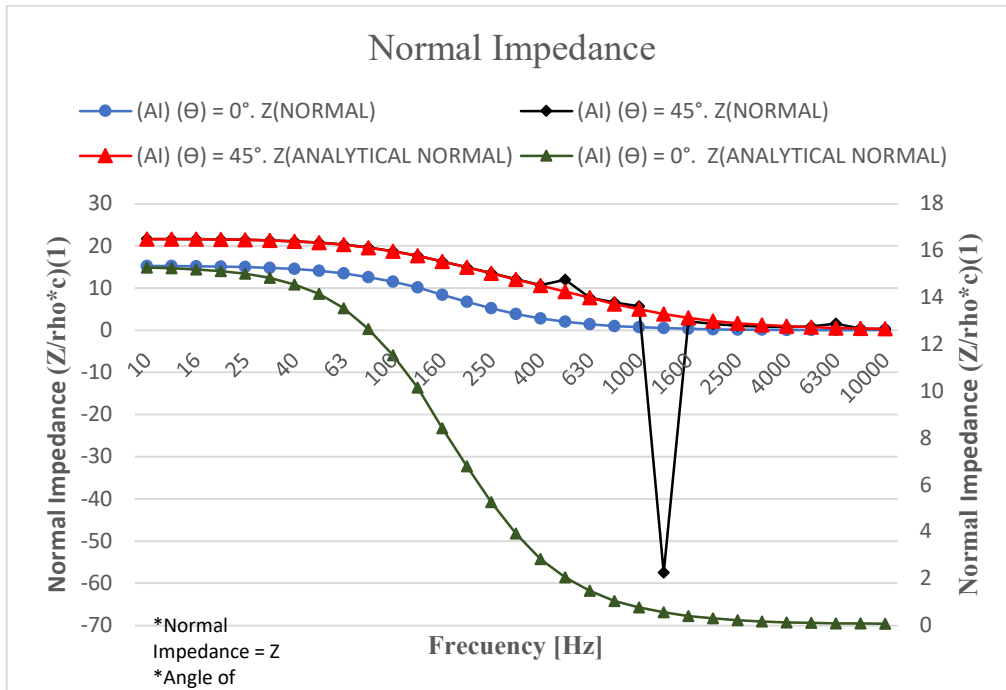


Figure 15. Normal impedance of the sample B2, with the different angles of incidence

### Absorption coefficient vs Frequency

The results of the absorption coefficient are shown in Figure 16, where the value of the absorption coefficient can be identified in the curve with an incidence angle of 45° ((AI) (Θ) = 45° α) of α = 0.96, f = 1.6 KHz, and α = 0.28, f = 10 KHz, corresponding to the linearization of the 45° incidence angle (analytical curve for the absorption coefficient with a 45° incidence angle (AI) (Θ) = 45° (α analytical)). This difference between these values is due to the variability of the curve, especially from 400 Hz onwards. It should be noted that the porosity of materials is an important factor in the simulations, which is why there is a considerable decrease in the value of the coefficient in the analytical curve at 45°.

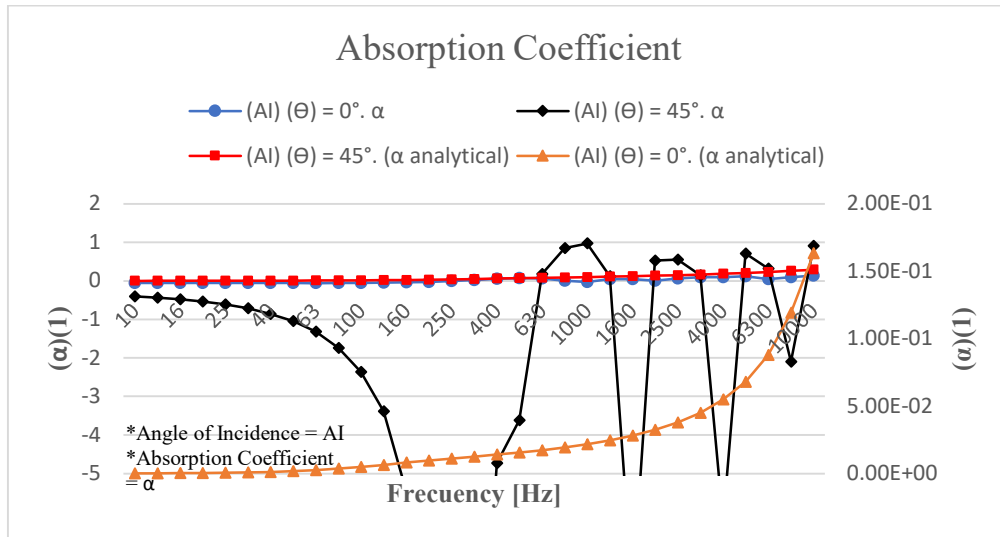


Figure 16. Absorption coefficient vs Frequency with the different angles of incidence.

#### 4. Discussion and conclusions

The tests carried out on the samples analyzed in the experimental design and acoustic simulations have generated the following discussion of results. When it comes to the density of construction materials, in this case, hollow concrete blocks, sample B1 has a lower density value of 205205 [kg/m<sup>3</sup>]. It should be noted that for the calculation of the density of this construction material, values of mass were considered when the material is completely dry and when it is fully saturated, i.e., submerged in water. These density values are an important parameter in the behavior of the material when the acoustic wave impacts it.

Porosity is a parameter that must be considered in the simulations of construction materials, as if a material is highly porous, it will allow the passage of the acoustic wave, and thus, it cannot be considered as soundproof. When analyzing the resulting data of the two samples, the following results are obtained for the hollow concrete blocks of samples B1 and B2, with porosity percentage values of 22.41 and 18.62. It is evident that the blocks have a higher percentage of porosity compared to other construction materials such as bricks, and therefore, simulations on this material have shown that they do not have great acoustic properties, affecting the value of the absorption coefficient.

The compression tests on the blocks allowed determining the value of the Young's modulus and the speed of sound, characteristics of great importance in carrying out acoustic propagation simulations. With these criteria, the following results were found sound velocity values of 2.24 and 2.71 [m/s], and 0.71 and 0.81 [m/s] for blocks B1 and B2, respectively. This parameter allows determining the acoustic impedance, of the samples studied, brick B2 has the lowest value with  $Z = 16.74$ , considering that this property analyzes the movement of particles in a medium.



The use of COMSOL Multiphysics software has allowed the realization of acoustic simulations of the construction material samples, using all the parameters obtained in the experimental phase, thus, the acoustic absorption coefficient could be calculated considering the incidence angle of the wave at  $0^\circ$  and  $45^\circ$  as critical angular values. This value will allow identifying which of the analyzed elements will behave in a better way as an acoustic inhibitor. The blocks have values of  $B1 = 0.97$  and  $B2 = 0.96$ , identifying that block B1 presents the best acoustic behavior, considering the maximum values generated when the sound wave is incident at an angle of  $45^\circ$ . For blocks  $B1 = 0.29$  and  $B2 = 0.28$ , from these results, the material that behaves best as an acoustic inhibitor is the common brick, compared to scientific literature, as it presents the most stable acoustic behavior.

COMSOL Multiphysics version 5.6 is the required computer tool for acoustic simulations since its versatility and intuitive handling have demonstrated high-quality results in this research. Through the 2D and 3D simulations on the construction materials, it was possible to find graphs of interest for analysis such as Pressure vs Frequency, Impedance vs Frequency, and Absorption coefficient vs Frequency in two-dimensional simulations, and Acoustic pressure, Sound pressure level, and Acoustic pressure, is surfaces in three dimensions.

Finally, it was possible to determine through experimentation and simulations that the studied construction materials, blocks, behave differently when the sound wave is incident on them, in this case, with a critical recommended incidence angle of  $45^\circ$ .

## 5. References

- [1] C. Velásquez, “DETERMINACIÓN DEL NIVEL DE CONTAMINACIÓN ACÚSTICA PRODUCIDO POR EL TRÁFICO VEHICULAR MEDIANTE MONITOREO AMBIENTAL EN LA CIUDADELA ‘VIEJA KENNEDY’ GUAYAQUIL,” 2023.
- [2] A. Marcotti F, B. Alvear V, A. Marcotti F, and B. Alvear V, “Pruebas de fusión auditiva y de detección de gaps: Evaluación de la resolución auditiva temporal,” *Revista de otorrinolaringología y cirugía de cabeza y cuello*, vol. 79, no. 2, pp. 248–260, Jun. 2019, doi: 10.4067/S0718-48162019000200248.
- [3] OECD (Organisation for Economic Co-operation and Development), “Home page - OECD,” 2022. <https://www.oecd.org/> (accessed Mar. 21, 2023).
- [4] OMS, OMM, and PNUMA, “Cambio climático y salud humana-Riesgos y respuestas RESUMEN OMS OMM PNUMA,” 2023.
- [5] Observatorio de Salud y Medio Ambiente, Unión Europea, and Gaes, “El Informe ‘Ruido y Salud’ se presenta con motivo del Día Mundial contra el Ruido,” *Ecodes*, 2012. <https://archivo.ecodes.org/web/noticias/el-informe-ruido-y-salud-se-presenta-con-motivo-del-dia-mundial-contra-el-ruido> (accessed Mar. 21, 2023).

- [6] A.-E. CREȚU, “FACADE OF PERFORATED PLATE: ANALYSIS OF ITS ACOUSTIC BEHAVIOR,” *SCIENTIFIC RESEARCH AND EDUCATION IN THE AIR FORCE*, vol. 18, no. 1, pp. 317–322, 2016, doi: 10.19062/2247-3173.2016.18.1.43.
- [7] A. Arjunan *et al.*, “Sound frequency dependent mesh modelling to simulate the acoustic insulation of stud based double-leaf walls Crashworthiness and energy absorber design View project Additively manufactured functional biomaterials for bone reconstruction View project Sound frequency dependent mesh modelling to simulate the acoustic insulation of stud based double-leaf walls,” 2014, Accessed: Mar. 21, 2023. [Online]. Available: <https://www.researchgate.net/publication/330667963>
- [8] E. Nacional de Sanidad Instituto de Salud Carlos III, *Efectos del ruido urbano sobre la salud: Estudios de análisis de series temporales realizados en Madrid*. 2021. doi: 10.4321/repisalud.5434.
- [9] L. Fiala, P. Konrád, J. Maděra, and R. Crný, “Data acquisition and acoustic modeling of heterogeneous building materials,” in *AIP Conference Proceedings*, Jul. 2019, vol. 2116, no. 1, p. 070006. doi: 10.1063/1.5114057.
- [10] R. Fediuk, M. Amran, N. Vatin, Y. Vasilev, V. Lesovik, and T. Ozbakkaloglu, “Acoustic Properties of Innovative Concretes: A Review,” *Materials*, vol. 14, no. 2, pp. 1–28, Jan. 2021, doi: 10.3390/MA14020398.
- [11] N. Holmes, A. Browne, and C. Montague, “Acoustic properties of concrete panels with crumb rubber as a fine aggregate replacement,” *Constr Build Mater*, vol. 73, pp. 195–204, Oct. 2014, doi: 10.1016/j.conbuildmat.2014.09.107.
- [12] M. Pereira, J. Carbajo, L. Godinho, J. Ramis, and P. Amado-Mendes, “Improving the sound absorption behaviour of porous concrete using embedded resonant structures,” *Journal of Building Engineering*, vol. 35, p. 102015, Mar. 2021, doi: 10.1016/j.job.2020.102015.
- [13] T. J. Cox and P. D’Antonio, “Book Review: Acoustic Absorbers and Diffusers: Theory, Design and Application,” *Building Acoustics*, vol. 12, no. 4, pp. 293–294, Dec. 2005, doi: 10.1260/135101005775219076.
- [14] G. Ciaburro and G. Iannace, “Numerical simulation for the sound absorption properties of ceramic resonators,” *Fibers*, vol. 8, no. 12, pp. 1–16, Dec. 2020, doi: 10.3390/fib8120077.
- [15] J. kun Huang, X. wei Liu, X. hua Chen, and H. jun Xiang, “Multiple flexural-wave attenuation zones of periodic slabs with cross-like holes on an arbitrary oblique lattice: Numerical and experimental investigation,” *J Sound Vib*, vol. 437, pp. 135–149, Dec. 2018, doi: 10.1016/j.jsv.2018.09.016.
- [16] R. Ibragimov and R. Fediuk, “Improving the early strength of concrete: Effect of mechanochemical activation of the cementitious suspension and using of various superplasticizers,” *Constr Build Mater*, vol. 226, pp. 839–848, Nov. 2019, doi: 10.1016/j.conbuildmat.2019.07.313.
- [17] G. A. Cravero, M. D. Flores, L. Budde, and C. Longoni, “Medición y simulación de tiempo de reverberación y otros parámetros acústicos de aulas,” *Mecánica Computacional*, vol.

- XXXII, no. 34, pp. 19–22, 2013, Accessed: Mar. 22, 2023. [Online]. Available: <http://venus.santafe-conicet.gov.ar/ojs/index.php/mc/article/view/4526>
- [18] S. Park, “Vibro-acoustic numerical simulation for analyzing floor noise of a multi-unit residential structure,” *Applied Sciences (Switzerland)*, vol. 9, no. 20, p. 4289, Oct. 2019, doi: 10.3390/app9204289.
- [19] Z. Xu, W. He, F. Xin, and T. J. Lu, “Sound propagation in porous materials containing rough tubes,” *Physics of Fluids*, vol. 32, no. 9, p. 093604, Sep. 2020, doi: 10.1063/5.0017710.
- [20] NTE INEN 638, “NTE INEN 638 BLOQUES HUECOS DE HORMIGÓN. DEFINICIONES, CLASIFICACIÓN Y CONDICIONES GENERALES. HOLLOW BLOCKS OF CONCRETE. DEFINITIONS, CLASSIFICATION AND GENERAL CONDITIONS,” 2010.
- [21] NTE INEN 638, “Bloques Huecos de hormigón. Definiciones, Clasificaciones Y Condiciones,” *Norma Técnica Ecuatoriana*, vol. 2332, no. 1, pp. 1–5, 2002.
- [22] INEN 857, “Áridos. Determinación de la Densidad Relativa (Gravedad Específica) y Absorción del Arido Grueso. INEN 857,” *INEN 857*, vol. 1, no. Primera Edición, pp. 1–14, 2010.
- [23] NTE INEN 857:2010, “Instituto Ecuatoriano de Normalización Norma Técnica Ecuatoriana NTE INEN 857:2010 Determinación de la densidad, densidad relativa (gravedad específica),” 2010.
- [24] NTE INEN 573, “Ecuatoriana Nte Inen 2854,” *NTE INEN 573*, no. VEHÍCULOS DE TRANSPORTE DE PASAJEROS INTRARREGIONAL, INTERPROVINCIAL E INTRAPROVINCIA. REQUISITOS, p. 34, 2015.
- [25] N. Técnica Ecuatoriana, M. Refractarios, D. De, L. A. Porosidad, A. De Agua, and D. Aparente, “MATERIALES REFRACTARIOS DETERMINACIÓN DE LA POROSIDAD ABSORCIÓN DE AGUA Y DENSIDAD APARENTE INEN 573”.
- [26] NTE INEN 3049, “NTE INEN 3049-2019. Ladrillos cerámicos. Parte 5: Métodos de ensayo,” *NTE INEN 3049*, 2019.
- [27] NTE INEN 3049, “Equipos de protección individual contra caídas. Cuerdas trenzadas con envoltura, semiestáticas. Requisitos y métodos de ensayo,” 2015.
- [28] NTE INEN 3066, “NTE INEN 3066: Bloques de hormigón, requisitos y métodos de ensayo. Servicio Ecuatoriano de Normalización,” p. 27, 2016.
- [29] NTE INEN 3066, “Norma Técnica Ecuatoriana Obligatoria BLOQUES HUECOS DE HORMIGÓN REQUISITO INEN 3066,” 2016. Accessed: Mar. 22, 2023. [Online]. Available: <http://181.112.149.204/buzon/normas/643.pdf>
- [30] NTE INEN 2619:2012, “BLOQUES HUECOS DE HORMIGÓN, UNIDADES RELACIONADAS Y PRISMAS PARA MAMPOSTERÍA. REFRENTADO PARA EL ENSAYO A COMPRESIÓN,” 2012.
- [31] COMSOL Multiphysics Reference Manual, “COMSOL Multiphysics Reference Manual,” 2019. [Online]. Available: [www.comsol.com/blogs](http://www.comsol.com/blogs)
- [32] T. COMSOL, “Comsol Benefits,” *COMSOL, Team*, 2020.

- [33] COMSOL, “COMSOL Multiphysics® v. 5.4 Reference Manual,” p. 1622, 2018.
- [34] H. González, S. Hellwig, and J. A. Montoya, “Resultados del ensayo del módulo de Young y resistencia a la flexión de vigas laminadas de *Guadua angustifolia* Kunth.,” *Scientia et Technica*, vol. XIV, no. 40, pp. 291–296, 2008, doi: 10.22517/23447214.3057.
- [35] L. A. Lancón Rivera, “Caracterización de la absorción sonora en modelos físicos a escala,” 2012. doi: 10.16/CSS/JQUERY.DATATABLES.MIN.CSS.
- [36] Antoni Carrión Isbert, “Diseño acústico de espacios arquitectónicos.” [https://books.google.com.ec/books?hl=es&lr=&id=mceSsNa6U3IC&oi=fnd&pg=PA20&dq=Carrión,+A.+\(n.d.\).+Diseño+acústico+de+espacios+arquitectónicos.&ots=hD4NWNHV4J&sig=gOYhSPI2wYu73ngTa24JELbYsYw&redir\\_esc=y#v=onepage&q=Carrión%2C+A.+\(n.d.\).+Diseño+acústico+de+\(accessed+Mar.+23,+2023\).](https://books.google.com.ec/books?hl=es&lr=&id=mceSsNa6U3IC&oi=fnd&pg=PA20&dq=Carrión,+A.+(n.d.).+Diseño+acústico+de+espacios+arquitectónicos.&ots=hD4NWNHV4J&sig=gOYhSPI2wYu73ngTa24JELbYsYw&redir_esc=y#v=onepage&q=Carrión%2C+A.+(n.d.).+Diseño+acústico+de+(accessed+Mar.+23,+2023).)
- [37] J. Torres, M. Petite, J. Carbajo San Martín, E.-G. Segovia-Eulogio, and J. Ramis-Soriano, “Caracterización de la impedancia de transferencia de materiales porosos-fibrosos usando holografía acústica de campo cercano (NAH),” 2014, Accessed: Mar. 23, 2023. [Online]. Available: <http://rua.ua.es/dspace/handle/10045/46005>
- [38] Lancón L, “EN MODELOS FÍSICOS A ESCALA Laura Angélica Lancón Rivera,” 2012.
- [39] I. 266 NTE, “EX,” 2014.
- [40] C. AB, “Acoustics Module,” *Acoustics Module, Interfaces*, p. 214, 2010.
- [41] P. A. COMSOL, “Porous Absorber,” *COMSOL, Porous Absorber*, pp. 1–22, 2012.
- [42] J. Gaïbor, “Desarrollo, Elaboración y Caracterización de un material compuesto con base de materiales reciclados para la fabricación de ladrillos destinados a mamposterías con propiedades de aislamiento acústico,” Escuela Superior Politécnica de Chimborazo, 2021.